SMART-1

AMIE

*A*dvanced *M*oon micro-*I*mager *E*xperiment

Document title:	**Test of the AMIE frame kernel V1**
Document number:	**S1-AMIE-RSSD-TN-008**
Issue/Revision:	**1/-**
Date:	**2007-Jul-03**

	Function	**Name**
Prepared by	AMIE Liaison Scientist	Björn Grieger
	AMIE Co-I	Detlef Koschny
		Jose Luis Vázquez García
	AMIE Co-I	Miguel Almeida

Document change record			
Iss./Rev.	Date	Pages affected	Description
D	2007-Apr-19	All	Placeholder put on Livelink
D/a	2007-Apr-19	1–5	Applicable text
D/b	2007-Apr-20	5–8	Draft basically completed
1/-	2007-Jul-02	All	Completely rewritten for V1 instead of V09

Contents

1 General items

1.1 Scope

The SMART-1 spacecraft contains a number of scientific instruments, a few of them being remote sensing instruments. One of them is the Advanced Moon Imaging Experiment (AMIE), a camera with 5.4° field of view and a total of 8 fixed filters in front of its CCD detector. This Technical Note addresses the frame kernel '`SMART1_V1.TF`' and the clock kernel '`SMART1_070227_STEP.TSC`' which are used with SPICE to map AMIE images to real world coordinates. We describe some tests which we conducted with these kernels. The tests do only address the description of the AMIE camera frames in the kernel '`SMART1_V1.TF`' and no other components of the SMART-1 spacecraft.

1.2 Introduction

The AMIE frame kernel defines for each of the individual filter frames the transformations which are needed to align the filter frame coordinate system with the spacecraft coordinate system. The AMIE clock kernel defines the transformation from the spacecraft clock count to ephemerids time. Both kernels are needed to map a filter frame image to real world coordinates, e. g., to map a Moon image to selenographic coordinates on the Moon's surface. Problems have been reported in matching AMIE images which have been mapped to the Moon's surface with known surface features. However, these problems have been found using older versions of frame and/or clock kernels.

Former tests have shown that the frame kernels '`SMART1_V08.TF`', '`SMART1_V09_version_A.TF`', and '`SMART1_V09_version_B.TF`' are erroneous and yield qualitatively wrong results. The first kernel implies a spurious transposition (exchange of x- and y-axies) while the latter two kernels imply a spurious rotation by 180°. The kernel '`SMART1_V09.TF`' provides correct image orientation, but the missalignment of the camera with respect to the SC z-axis is incorrectly described. The older clock kernel '`SMART1_051207_FAKE.TSC`' implies considerable time deviations which can lead to a spatial shift of about 20° in selenographic coordinates.

1.3 Brief summary of results

Herein, we demonstrate that the spacecraft frame kernel '`SMART1_V1.TF`' correctly represents the AMIE filter frames within the accuracy of current knowledge on the camera geometry. Furthermore, when used together with the spacecraft clock kernel '`SMART1_070227_STEP.TSC`', AMIE images projected onto the Moon's surface match images and maps from other sources with a deviation of less than 10 pixels.

1.4 Reference documents

S1-AMIE-RSSD-TN-001 AMIE detector orientation in s/c coordinate system (Iss./Rev. 1d, 2004-Jan-30)

S1-AMIE-RSSD-TN-004 AMIE boresight analysis (Iss./Rev. 1a, 2007-Feb-28)

1.5 Abreviations

AMIE	Advanced Moon Imaging Experiment
API	Application Programming Interface
CCD	Charge Coupled Device
FOV	Field Of View
SC	Spacecraft
SPICE	Spacecraft, Planet, Instrument, Camera-matrix, Events
SOPS	Science Operations Planning System

2 Transform all filter FOVs to the space craft frame

This test addresses only the frame kernel '`SMART1_V1.TF`' and is independent of any clock kernel. The idea is to compute with SPICE — using the frame kernel '`SMART1_V1.TF`' — the projection of the fields of view (FOVs) of all filter frames on a screen in front of the SC, perpendicular to the SC z-axis with the SC z-axis pointing to the origin of the screen coordinates. By inspecting this projection we can verify the relative position of the FOVs of all filters with repect to each other and also the missalignment between the boresight of the AMIE CCD frame and the SC z-axis. The projection is performed in three steps which are described in the following sections.

2.1 Get vectors pointing in the directions of the boresight and the four corners of the FOV for each filter

For each filter frame of AMIE, we use the SPICE API `getfov` to compute vectors pointing along the boresight and along the viewing direction of the four corners of the FOV. It is important to note that these are not unit vectors; their length is not specified beyond "non zero". The vectors are specified in the native frame of each respective filter. In this test, we do not care how the vectors look like in their native frames and how the transformation of the individual filer frames to the (parent) CCD frame is described. We will only check the FOVs of the filters and the complete CCD once they are transformed to the SC frame.

2.2 Transform the FOVs to the space craft frame

We transform the vectors from their native filter frames to the SC frame using the SPICE APIs `pxform`, which provides a respective rotation matrix, and `mxv`, which applies the rotation matrix to a vector. After this operation, we have vectors given in the SC coordinate system [S1-AMIE-RSSD-TN-001] pointing along the boresights and along the corners of the FOVs for all filters.

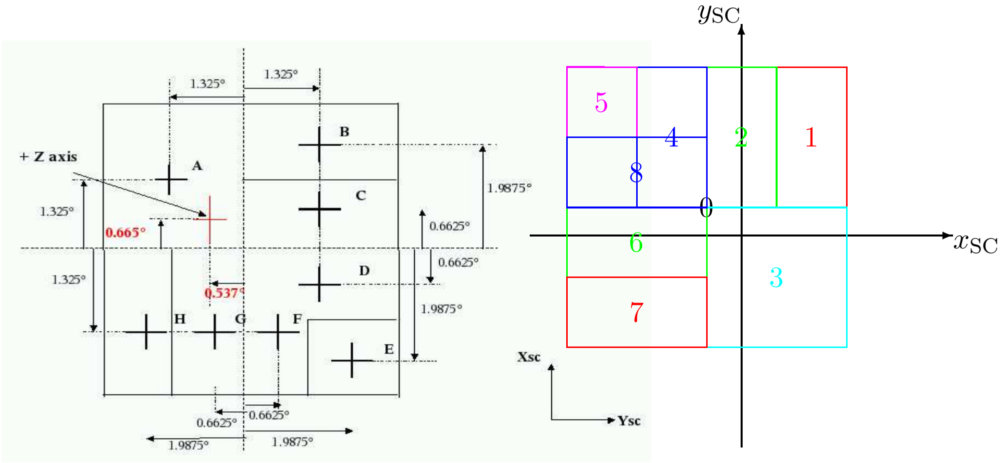

From Scenario Parameter List Plot with new kernel

Figure 1: Comparison of the filter FOVs according to the Scenario Parameter List and as plotted with the new instrument frame kernel. Note that the axes of the two repective co-ordinate systems are inverted.

2.3 Plot the x and y co-ordinates of the transformed vectors in the x_{SC}-y_{SC}-plane

As noted above, the length of our vectors is unknown. We now scale all vectors so that their z-component becomes unity. To obtain the viewpoints of all vectors on a screen which is located one unit length in front of the SC, we just have to take the x- and y-components of the vectors. A plot of all FOVs is presented on the right hand side of Fig. 1. We have plotted the number of each filter at the borsight position and lines joining the corners of the field of view in different colors for the different filter (well, not quite, filter 1 and 7, 2 and 6, and 4 and 8, respectively, share the same color). The filters are plotted in the sequence given by their number. Note how the right FOV edge of filter 2 covers the left FOV edge of filter 1, etc.

For comparison, we show the filter FOVs in SC co-ordinates as defined by the Scenario Parameter List (copied from [S1-AMIE-RSSD-TN-004]) on the left hand side of Fig. 1. Note that x- and y- axes have to be swapped to match one to the other. We did not swap the axes within our plotting code to avoid to introduce an error here. We just plainly ploted x and y computed as described above. Therefore the swapping is left to the imagination of the reader. Taking it into account, we observe the following:

- The edges of the individual filter frames fit together correctly.
- The relative orientation of the filters with respect to each other is correct.
- The missalignment given by the position of the SC z-axis — i. e., the origin of the co-ordinate system — within the CCD frame is correct.

3 Compute right ascension and declination of the NONE filter boresight during Vega pointing

On 2004-Mar-26 from 07:03:20 to 07:12:40, the boresight of the NONE filter was pointed to Vega (information from SOPS). An image taken during Vega pointing is shown in Fig. 2. The image of vega is indeed located very close to

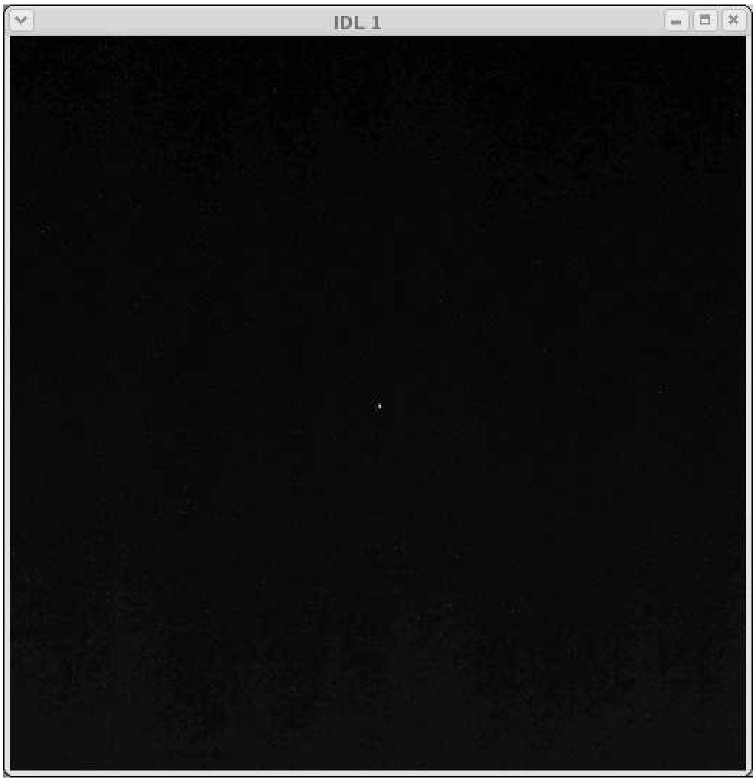

Figure 2: Image '`AMI_EAE3_040326_00068_01000.IMG`' of Vega in the NONE filter frame.

the center of the NONE filter area of the CCD; it is about two pixels away from the center [S1-AMIE-RSSD-TN-004]. The small offset reflects that the boresight of AMIE was not known exactly when the pointing was conducted. In fact, as we perform the test described herein, the boresight is still not known more exactly. Our frame kernel uses the same offset angles which where used to determine the pointing. Therefore, if the kernel is correct, we expect that the boresight as given by SPICE does exactly point to Vega during Vega pointing. The correction of the small observed offset will be included in a future version of the kernel that may also take into account geometric distortion.

The test if the kernel does exactly reproduce the Vega pointing is straight forward. Similarly to the test described before, we use SPICE to compute the boresights of all filters in their own native frames. Then we transform these vectors to the J2000 frame. At this point, the clock kernel is needed to determine the SC attitude at the time of Vega pointing, however, the accuracy requirement is not very high as the pointing was constant for several minutes. We arbitrarily chose a time point well within the time range of commanded Vega pointing, 2004-Mar-26, 07:05:00. The time when the image was really taken was not available in the current version of the AMIE data set (‘`S1-X-AMIE-2-EDR-RAW-V1.0`’). From the boresight vector in the J2000 system, we compute right ascension and declination of the boresights of all filters and plot these together with the position of Vega, see Fig. 3. We note the

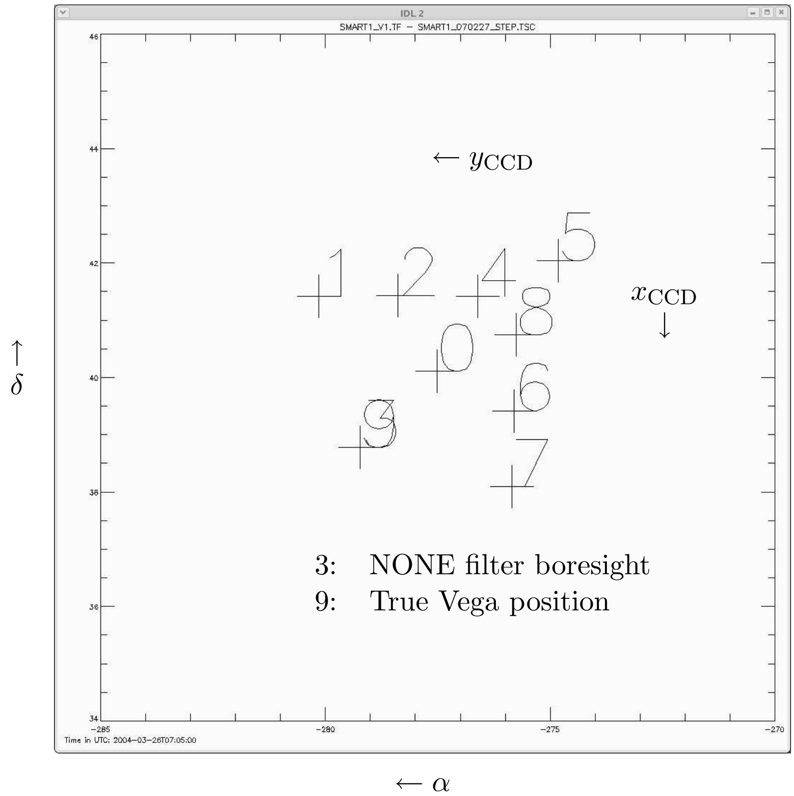

Figure 3: Boresights of the AMIE filter frames (1–8) and the true position of Vega (9). Right ascension is plotted negative to have it increasing from right to left and get real world orientation.

following:

- The relative positions of the filter boresights with respect to each other are correct (The figure provides real world orientation).
- The two crosses marking the NONE filter boresight and the Vega position fall exactly on top of each other.

4 Project a combined image onto the Moon's surface

4.1 Get the viewing directions of the corners of the FOV of the complete CCD frame

Again smilarly as described above, we compute vectors pointing along the corners of the FOV of the complete CCD frame and also the boresights of the individual filter frames. SPICE provides these vectors in the CCD's own frame, and here we tranform them into the fixed Moon reference frame `IAU_MOON`.

4.2 Compute the intersections of these viewing directions with the Moon's surface in longitude and latitude

Besides the viewing directions of boresights and FOV corners, we also need the position of the SC in the Moon frame (computed with the SPICE API `spkpos`) and the radius of the Moon (computed with `bodvar`). Given all this, we use `surfpt` to compute the intersections of the lines of sight with the moon surface and transform them from cartesian co-ordinates to latitude and logitude.

4.3 Relate the FOV corners on the Moon to the respective corners of the combined image

Herein, we will base the projection of an combined image only on the position of the corners of the complete CCD frame. However, we have also projected the boresights of all filters onto the Moons surface. The reason is that we originally did not know which of the four corner vectors provided by SPICE belongs to which corner of the image. Inspecting the positions of the boresights on the Moon's surface clarifies the orientation of the combined image, cf. Fig. 4.

4.4 Plot the image in longitude and latitude

We plot the image by placing the corners at their computed positions in latitude and longitude and linearly interpolating all pixels in between. The result is shown in Fig. 4. This interpolation introduces some distortion, as in principle each pixel has to be projected individually. However, the image is not located two far from the equator, so that this distortion is moderate and probably not larger than the geometric distortion due to the camera which is not yet taken into account anyway.

4.5 Comparison with the Lunar Map Series

We compare the projected AMIE image with a map from the Lunar Map Series available at

`http://www.lpi.usra.edu/resources/mapcatalog/LM/`

This series was compiled from Apollo images. Figure 5 illustrates the coverage. A map of Mare Serenitati from this series is shown in Fig. 6. The AMIE image is located close to the right edge of this map. In Fig. 7 we compare

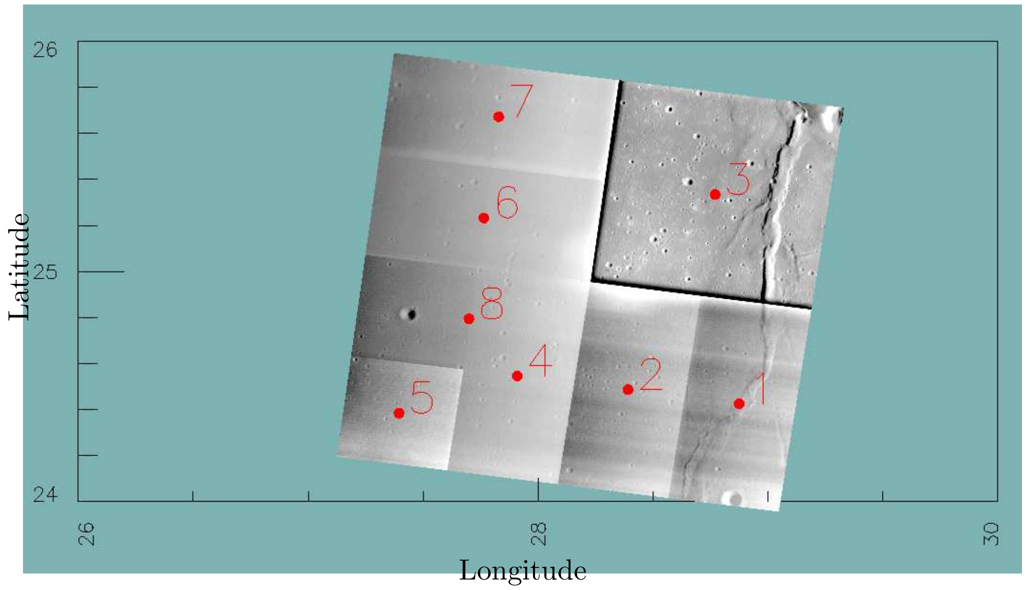

Figure 4: Combined image '`AMI_MAE*_002735_00014_00023.IMG`' projected onto the Moon's surface. Red dots indicate the boresights of the individual filter frames.

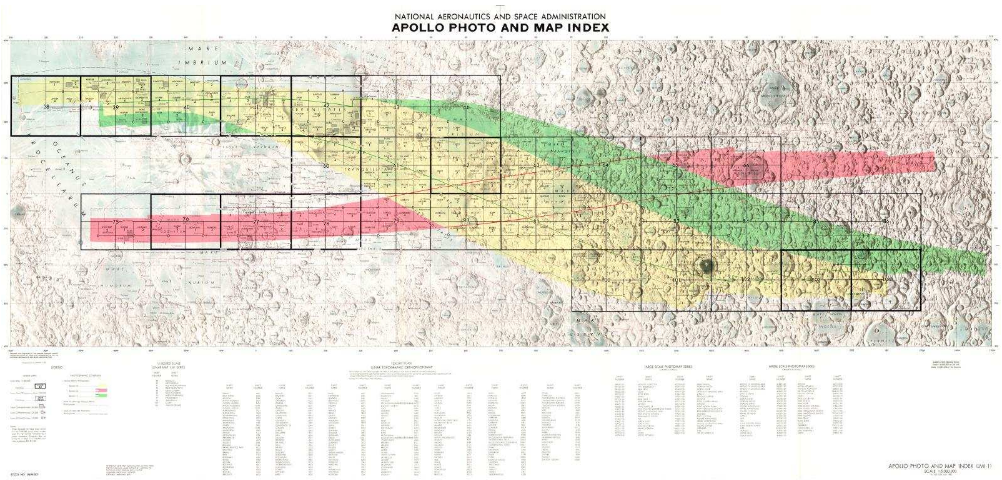

Figure 5: Coverage of the Lunar Map Series.

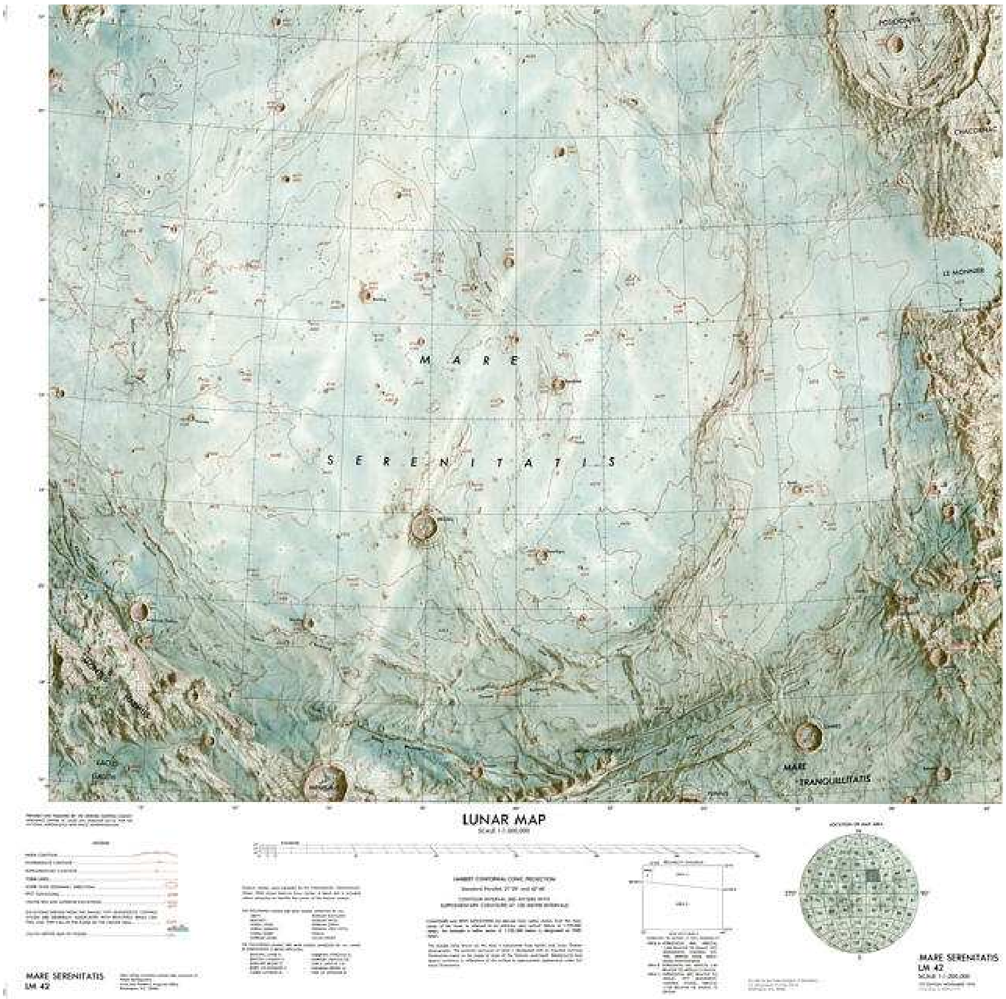

Figure 6: Map of Mare Serenitati (LM-42) from the Lunar Map Series.

the projected image with a cut out from the map. The AMIE image is shown in cylindric equidistant projection while the map is in sterographic projection. This introduces some distortion, but as we are not too far from the equator it should not be large. The amount of distortion is illustrated by the curvature of the latitude circles, which are straight lines in the cylindric projection.

We note that the locations of major craters and of the ridge at the eastern edge match quite well.

4.6 Comparison with Clementine

The Clementine basemap is available in cylindric equidistant projection at

`http://www.nrl.navy.mil/clm/`

With a provided Tool Panel, one can specify the desired resolution and the center co-ordinates of an image. The center is marked with a white cross. This allows us to exactly superimpose an AMIE image onto a Clementine image, see

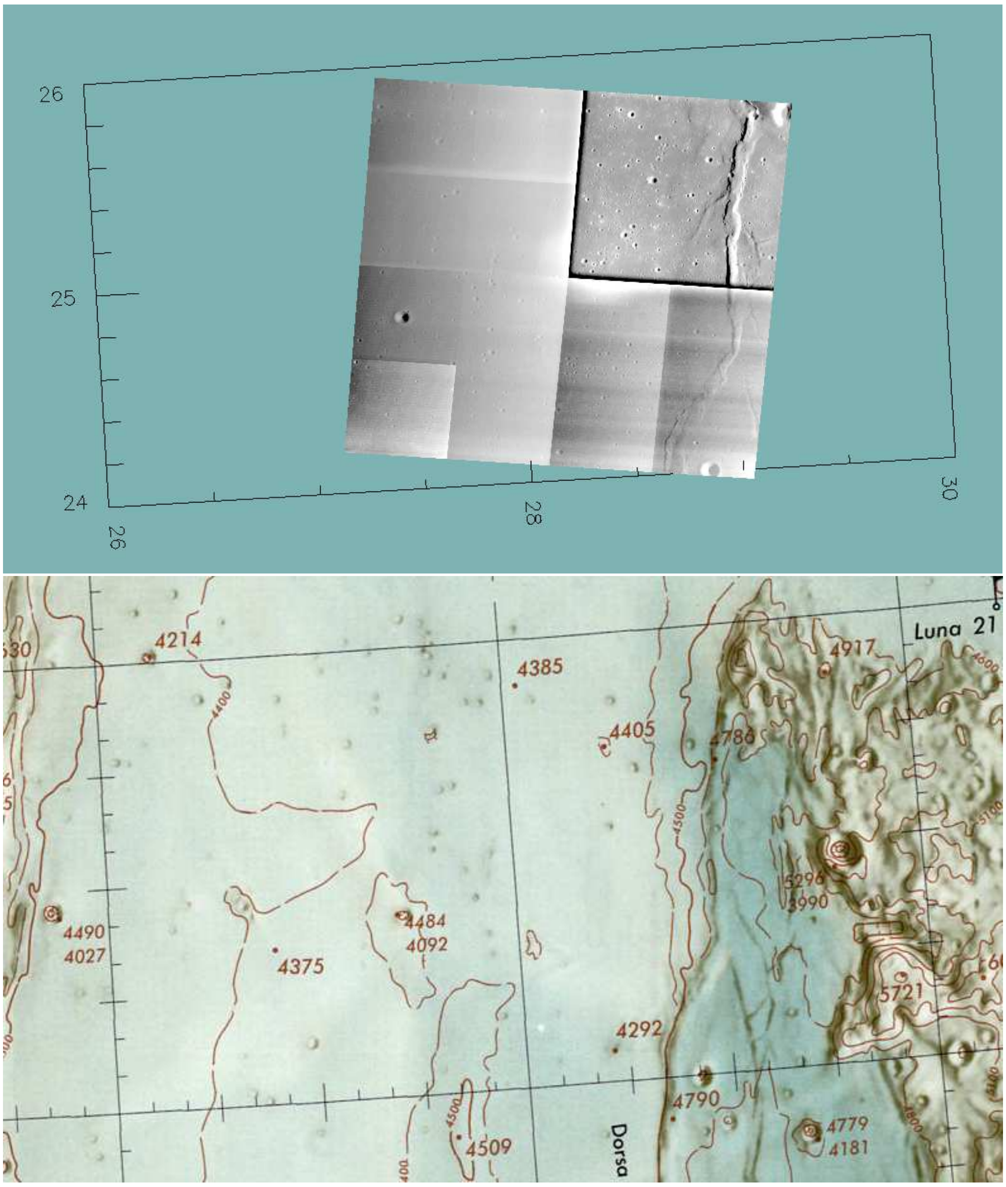

Figure 7: Comparison of the projected AMIE image with the Map from the Lunar Map serie.

Fig. 8. Again we see that the major features match quite well. If we look more into the details, we notice small deviations of up to 10 pixels. For the time being, this is a reasonable accuracy. Further investigations will show whether these deviations are due to geometric distortion of the camera or inaccuracies of the SC clock kernel.

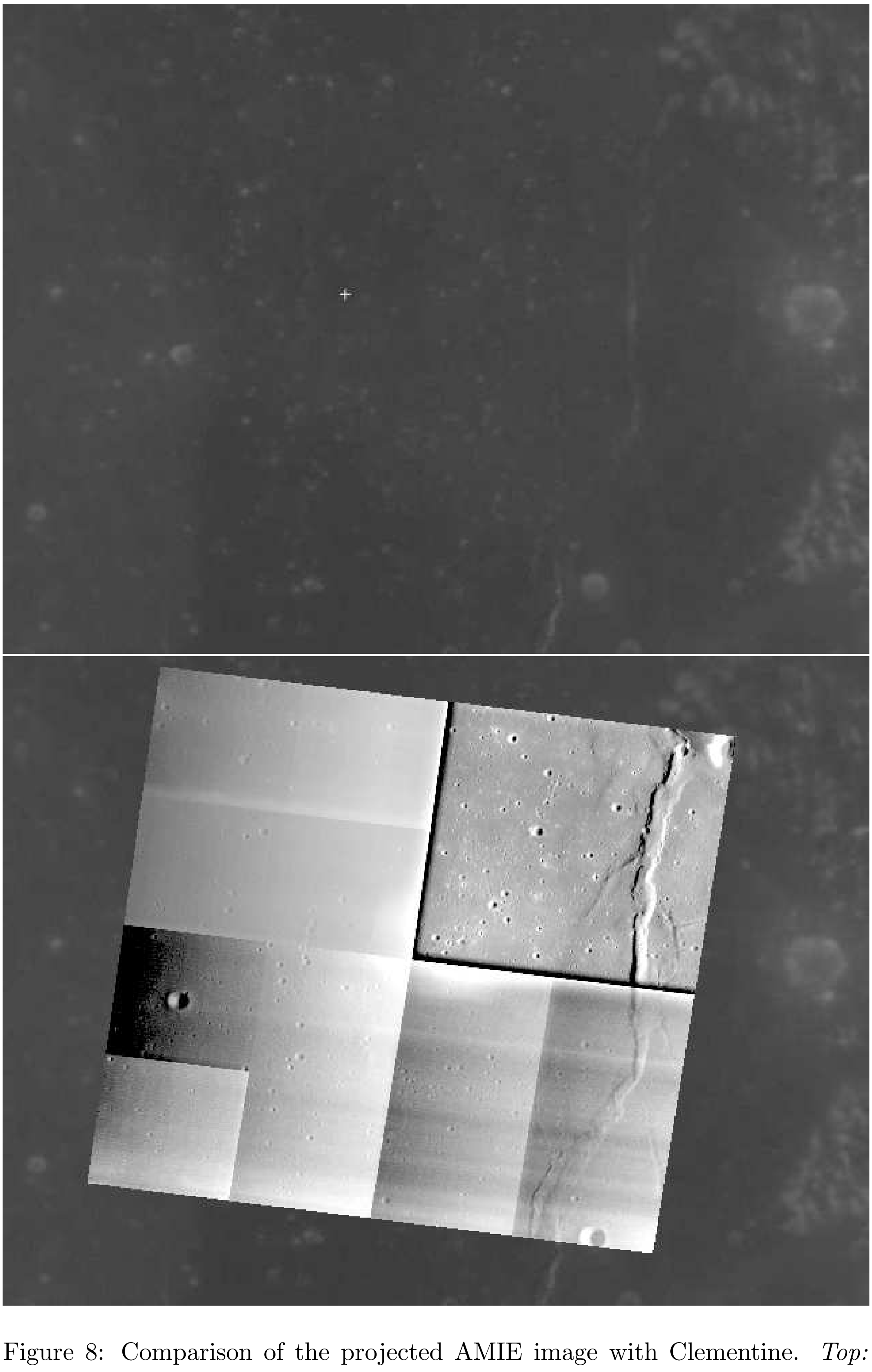

Figure 8: Comparison of the projected AMIE image with Clementine. *Top:* Only Clementine. *Bottom:* Clementine with AMIE image superimposed.